Programmable, Pattern-Memorizing Polymer Surface

*Zhen Wang, Curt Hansen, Qi Ge, Sajjad H. Maruf, Dae Up Ahn, H. Jerry Qi, and Yifu Ding**

Shape-memory polymers (SMPs) memorize and recover their permanent shapes with their strain levels up to a few hundred percent. This unique capability enables significant, potential applications ranging from surgical stents and sutures,[1] temperature sensors,[2] and aerospace deployable structures.[3] However, all current SMP applications focus on harvesting the macroscopic scale deformation, i.e. employing the SMP as structural materials. An intriguing capability of all SMPs, which remains largely unexplored, is their ability to memorize and recover nanoscale patterns or structures. Here we demonstrate that SMPs can memorize and faithfully recover their lithographically fabricated, permanent or even temporary surface patterns. More significantly, tunable multi-pattern memory capability can be achieved in Nafion films. Considering the prevalence of nanostructured surfaces in emerging nanotechnologies, such pattern-memorizing surfaces could potentially transform these technologies.

During a typical shape memory cycle, an SMPs permanent shape is first "programmed" into a temporary shape under mechanical loading at a temperature higher than the transition temperature (either glass transition temperature, T_g, or melting temperature, T_m) of the SMP. At the permanent shape, the polymer chains between crosslinking points can be considered at the equilibrium state, or the lowest energy state. The mechanical loading during the programming deforms the chains into a higher energy state (with lower entropic freedom), forming the temporary shape. Without the mechanical constraints, the SMP sample will return to their permanent shape to minimize the system energy. However, this temporary shape can be "fixed" as the temperature decreases below the T_g (or T_m) of the SMP before releasing the mechanical loading and remains stable indefinitely. The SMP softens and recovers its permanent shape when exposed to an environmental stimuli such as heat,[4,5] light,[1] or even solvent vapors.[6] During the recovery, strain or stress can be harvested under free or constrained conditions, respectively.[7,8] However, beyond such structural applications, the potential applications of SMP surfaces have yet to be explored.

King et al. reported that AFM-indented holes on a SMP surface can be recovered via heating which enables the AFM-based data storage.[9,10] Recently, Burke et al. showed that micron scale patterns embossed on liquid crystalline elastomer can be erased upon annealing.[11] However, such hole or pattern recovery is not unique to SMPs. Any thermoplastic polymers are capable of surface leveling, driven by the minimization of surface energy.[12,13] In other words, all polymers have the tendency to smooth out their surfaces to reduce their surface energy, without involving the entropically-driven "shape memory" effect. Recoverable micro-protrusions on SMP were also achieved by combining indentation and surface polishing.[14,15] However, in this case, the recovered surface is different from the original permanent shape. Similar approach was used to create two-way pattern memory effect in shape memory alloys.[16] In this case, the pattern memory effect is driven by the phase transformation of the alloy, which only provides very limited deformation strain.

Here, we demonstrate the successful programming and recovery of a range of lithographically fabricated, dense SMP patterns via Nanoimprint Lithography (NIL). NIL is a simple and reliable fabrication approach capable of creating sub-10 nm features at low cost.[17–19] There are two types of NIL processes: thermal embossing NIL (TE-NIL), and step-and-flash NIL (SF-NIL). In a TE-NIL, a polymer film is squeezed into the cavities of a rigid mold (typically Si) under relatively high pressure (few MPas) and temperature ($T > T_g$). A replica is then created after the mold separation at $T < T_g$. Such a TE-NIL process is essentially a combination of "programming" and "fixing" steps in a typical shape memory cycle, but at much smaller length scales. In comparison, SF-NIL is mostly carried out at room temperature with UV radiation which crosslinks reactive monomers to replicate the mold.

First, we examine the pattern memory effect using an acrylate-based SMP that has a T_g around 95 °C (Figure S1).[20] The flat surface of the SMP film (permanent shape) was programmed with TE-NIL into line-and-space grating patterns (temporary shape). After annealing at a temperature above T_g, the permanent flat surface recovered quickly. However, as mentioned, surface patterns of thermoplastic polymers also smooth out during thermal annealing.[12,13] Therefore, to demonstrate the unique pattern memory capability of SMPs, we fabricated line-and-space grating onto the SMP surfaces as their permanent shapes with identical pitch (Λ = 834 nm, a line-to-space ratio, R_{ls} = 1) but varying heights ($H_{permanent}$). The cross-sections of all SMP grating lines were sinusoidal-like, replicated via SF-NIL from sacrificial polyacrylic acid (PAA) molds, which were obtained by controlled thermal reflow of as-imprinted PAA patterns (see experimental and Figure S2).

We now demonstrate the novel capability of the pattern memory cycle (**Figure 1**) using an acrylate-based SMP with a permanent grating pattern, $H_{permanent}$ = 179 nm (Figure 1d and 1g), which displayed the strong diffractive color under white light illumination (Figure 1a). This permanent pattern was "programmed" using a flat Si wafer and TE-NIL at 180 °C under 4 MPa for 30 min. The pressurization of the wafer flattened the SMP surface which became "fixed" after the SMP

Z. Wang,[+] C. Hansen,[+] Q. Ge, S. H. Maruf,
Dr. D. U. Ahn, Prof. H. J. Qi, Prof. Y. Ding
Department of Mechanical Engineering
University of Colorado at Boulder
Boulder, CO 80309-0427, USA
E-mail: yifu.ding@colorado.edu
[+] Z.W. and C.H. contributed equally to this work.

DOI: 10.1002/adma.201101571

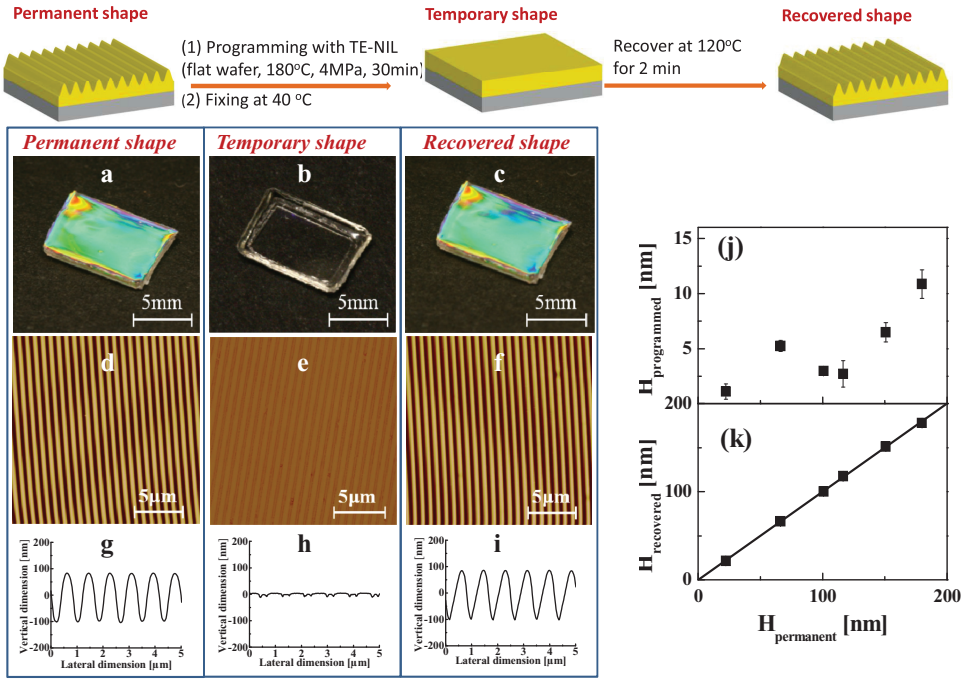

Figure 1. Pattern memory cycle in an acrylate-based SMP. Top: schematic illustration of the programming and recovery steps. (a)–(k) show the experimental characterization of the pattern memory cycle. Optical images of a patterned SMP (Λ = 834 nm, H = 179 nm) at different stages of the cycle: (a) permanent pattern; (b) after programming with a flat mold; and (c) recovered pattern. (d)–(f) are the topographic AFM images of (a)–(c), correspondingly, and (g)–(i) are the cross-sectional profiles of (d)–(f). (j) and (k) show the remaining pattern heights after programming ($H_{programmed}$) and the recovered pattern height ($H_{recovered}$) as a function of the permanent pattern height ($H_{permanent}$), respectively. For all samples, the programming was carried out via TE-NIL with a flat wafer at 180 °C under 4 MPa for 30 min. Error bars in (j) represent statistical averages of pattern heights obtained at 6 different locations on each sample and are smaller than the size of the symbols in (k).

cooled down to 40 °C before releasing the pressure. As a result, the programmed SMP no longer showed any diffractive color, but instead displayed sheer transparency (Figure 1b). From the AFM measurements, the pattern heights decreased to approximately 12 nm (Figure 1h and 1j). Such colorless SMP then quickly recovered its highly diffractive, permanent pattern after annealing for 2 min at 120 °C (Figure 1c). Similar to the analysis of bulk SMPs, the degree of pattern recovery (R_r) can be quantified as: $R_r = H_{recovered}/H_{permanent}$, where $H_{recovered}$ is the recovered grating height. From the AFM measurements (Figure 1f and 1i), both the $H_{recovered}$ (179 nm) and the cross-sectional profiles of the recovered pattern were identical to that of the permanent SMP pattern (Figure 1d and 1g), suggesting full pattern recovery.

Notably, the successful pattern memory cycles were achieved for all the 834 nm pitch SMP gratings with varying pattern heights ($H_{permanent}$ = 20, 65, 100, 120, 155, 179 nm) (Figure 1j and 1k). The experimental results showed that remaining pattern heights after the programming step ($H_{programmed}$) decreased progressively with decreasing $H_{permanent}$ (Figure 1j). However, regardless of $H_{programmed}$, 100% recovery was achieved for all patterns (Figure 1k). Furthermore, a smaller permanent pattern size (Λ = 150 nm, R_{ls} = 1, $H_{permanent}$ = 45 nm), fabricated using SF-NIL with a sacrificial PAA pattern, demonstrated the same successful pattern memorizing cycle as the Λ = 834 nm patterns (Figure S3). This smaller pattern size lies below the diffraction limit of visible light, accounting for its transparency throughout the cycle. The AFM measurements indicate the 150 nm pitch SMP pattern was flattened completely by TE-NIL at 180 °C under 4 MPa for 30 min (Figure S3b), but was recovered 100% after annealing for 2 min at 120 °C.

We systematically modeled the mechanical deformation of the 834 nm pitch SMP grating pattern during the TE-NIL flattening process, to examine the robustness of this process from the mechanics point of view (Figure S4). The simulation revealed that the stress required to flatten the grating pattern increased with the modulus of the SMP, $H_{permanent}$, and the elastic constraints from the substrate. Such constraints are negligible for all current samples due to their relatively large thickness (tens of microns).

To further investigate the pattern memory effect, the permanent SMP grating pattern was programmed using an additional Si grating mold (**Figure 2**). First, the permanent pattern on the acrylate-based SMP was fabricated using SF-NIL directly from a non-annealed PAA mold. The AFM scan detailed a trapezoidal cross-sectional profiles with a $H_{permanent}$ = 194 nm (Figure 2a). Then, this permanent pattern was subsequently programmed using TE-NIL at 180 °C under 4 MPa for 30 min, with the Si grating lines oriented perpendicularly to the SMP grating lines (Figure 2b). The effective pressure at the contact region is roughly 4 times the pressure applied on the Si mold, approaching approximately 16 MPa, and thereby compresses the rubbery SMP line into the 2D grid-like pattern (mechanical modeling result shown in Figure S5). After fixing at 40 °C, a temporary, grid-like pattern was created on the SMP surface, which differed from the regular 2D array gratings in which all

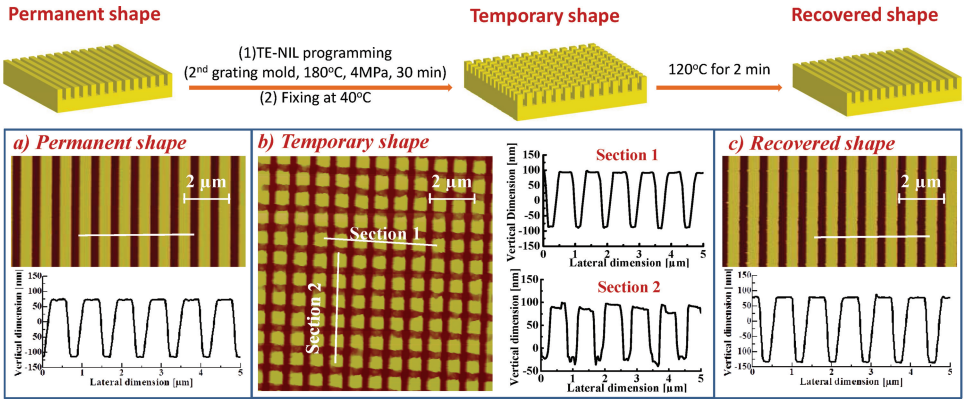

Figure 2. Top: schematic illustration of the pattern memory cycle in an acrylate-based SMP programmed with a second grating pattern. Bottom: topographic AFM image of the (a) permanent pattern, $\Lambda = 834$ nm, $R_{ls} = 1$, and $H_{permanent} = 194$ nm; cross-sectional profile of the pattern is shown below. (b) temporary 2D grid-like pattern programmed with a second grating pattern with grating lines perpendicular to the original lines. The cross-sectional profiles along the two marked section directions are shown on the right of the image. c) recovered line-and-space grating pattern after the sample was annealed at 120 °C for 2 min. Similarly, the cross-sectional profile displayed below the image, demonstrates 100% pattern recovery.

posts have identical geometries. Instead, it displayed highly anisotropic cross-sectional profiles along the two grating vectors: undulations of 185 nm (Figure 2b Section 1) and 100–110 nm (Figure 2b Section 2). After annealing for 2 min at 120 °C, the grid-like, temporary pattern recovered fully to its original line-and-space grating, permanent pattern (Figure 2c).

The pattern memory cycle in acrylate-based SMPs (Figure 1 and 2), as detailed above, exhibits a dual pattern memory effect, using a single programming step. Conventionally, the limiting factor for the number of temporary shapes that a given SMP can memorize is the discrete number of intrinsic transition temperatures of the SMP.[21] Therefore, to achieve multi-shape memory, a material or system containing multiple transition temperatures are necessary.[22–24] For example, polymer networks based on poly(ε-caprolactone) (PCL) and poly(cyclohexyl methacrylate) (PCLMA) exhibited a triple-shape memory effect, i.e. memorizing two temporary shapes,[22,23] due to their respective transition temperatures of PCL and PCLMA. Similarly, a triple-shape memory effect was also achieved in bilayer epoxy films because each layer has distinct T_g.[24] Intriguingly, Xie discovered that multiple shape memory can also be achieved in single component polymer such as Nafion, which has a broad glass-to-rubber transition zone.[21] Here we show that Nafion films can memorize three temporary patterns, i.e. displaying a quadruple pattern memory effect, by programming the deformation within its glass-transition zone (**Figure 3**).

Initially, the planar Nafion film, considered the permanent shape (Figure S6b), was programmed using TE-NIL at 180 °C under 4 MPa for 10 min, which produced the first temporary grating pattern ($\Lambda = 834$ nm, $R_{ls} = 1$, $H = 194$ nm) (Figure 3a), with trapezoidal cross-sections. This programming temperature significantly exceeds Nafion's glass-transition zone (Figure S7), and thus suggests that the deformation is predominantly viscous flow in the cavity filling. The second temporary pattern, a grid-like grating (Figure 3b), was produced using TE-NIL by orienting the Si grating lines perpendicular to the grading lines of the first temporary pattern at 90 °C under 4 MPa for 3 min, similar to grid-like pattern on the acrylate-based SMP (Figure 2b). As seen in Figure 3b, the pattern height along S1 remained ~190 nm and an undulation ~110 nm formed along S2, with a resultant depth ~80 nm along S3. In general, the curved cross-sectional profile along S2, the depth along S1, and the slight dilation exhibited by S3 (Figure 3b), collectively indicate that during this programming step, Nafion's deformation is predominately elastic. Additionally, the amplitude of the undulation represented by S2 (110 nm) equals the pattern height obtained using TE-NIL on the flat Nafion film at 90 °C using the same pressure, 4 MPa (Figures S6c and e).

A third, temporary pattern was programmed on the grid-like Nafion surface at 60 °C under 4 MPa for 30 min, using a 150 nm Si mold. Grating lines were oriented 45° with respect to the grid pattern's grating vectors (Figure 3c). This smaller grating was imprinted onto the elevated part of the grid pattern, but the pattern height produced was only 25 nm (Figure 3c) due to the significantly large modulus (100 MPa) of Nafion film (Figure S7). In addition, the average depths along S1 decreased from 190 nm to 105 nm and similarly decreased along S2 from 110 nm to 22 nm (Figure 3c). This suggests the dense Si mold, intended to create the 150 nm grating pattern, also inadvertently flattened the grid pattern. This compression causes the height reduction of the extruded part in the grid pattern, while minimally impacted the lower part of the grid pattern (S3) (80 nm to 70 nm). Such flattening effect resembles that shown in Figure 1, but the degree of flattening is much less dramatic because the higher modulus of Nafion at 60 °C. Note that such unintended flattening effect during multiple programming steps could bring significant difficulty in precisely controlling the desired highly hierarchical structures. Further separating the subsequent programming steps might be able to alleviate this problem. Since topographic AFM images are convolutions of the tip shape and the actual surface topography, we included the FE-SEM image of the patterned Nafion surface to illustrate the hierarchical patterning (Figure 3c).

Despite the complex deformation involved in the programming, successful recovery of the grid pattern resulted after annealing the Nafion film at 60 °C for 80 min (Figures 3c and 3d). The 150 nm pitch pattern almost disappeared. The recovered pattern height of S1 (185 nm) correlates to a 97% recovery;

ADVANCED MATERIALS
www.advmat.de

www.MaterialsViews.com

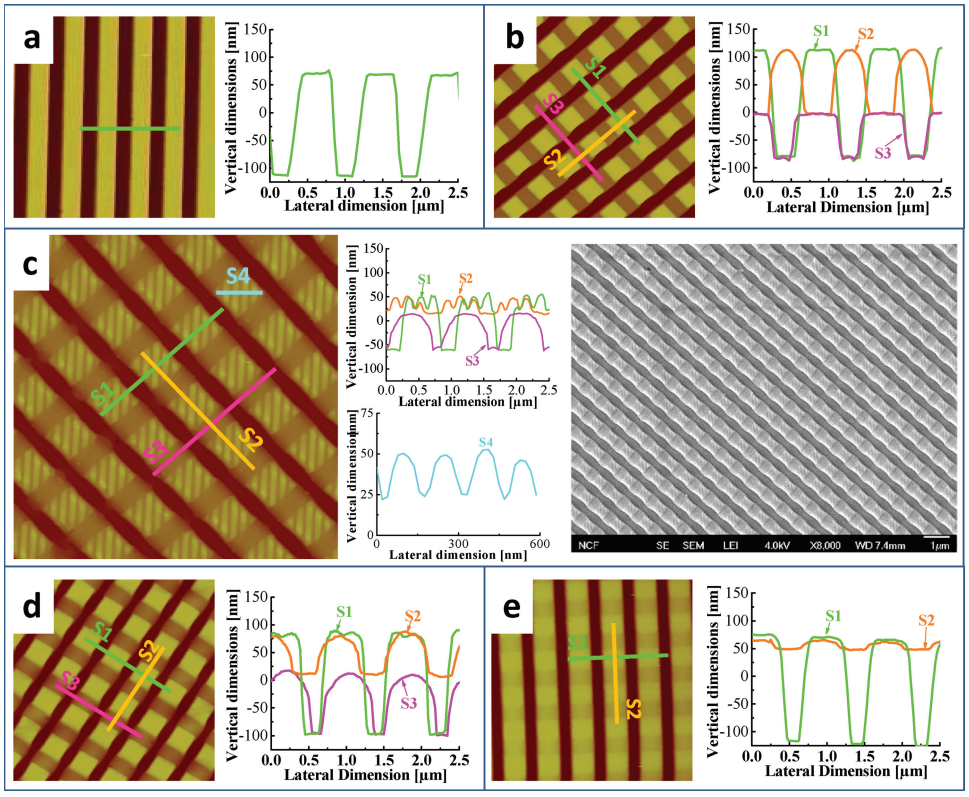

Figure 3. Topographic AFM images of multi-pattern memory effect in Nafion films programmed by TE-NIL. A flat Nafion film (permanent pattern, Figure S5b) was programmed into (a) a line-and-space grating at 180 °C for 10 min, with an 834 nm Si template, and then programmed into (b) a grid-like grating pattern at 90 °C for 3 min using the identical Si template but now oriented perpendicular to the Nafion grating. Finally the sample was programmed into (c) at 60 °C for 30 min with a 150 nm pitch template oriented 45° with respect to the previous patterned grating lines. Its FE-SEM image is shown on the right. After subsequent heating at 60 °C for 80 min, the Nafion surface recovered to (d). Additional heating at 90 °C for 10 sec resulted in (e). And finally, its smooth, permanent shape is recovered after 10 min at 190 °C (Figure S5b). All AFM images are 5 μm × 5 μm in size, with a depth scale of 400 nm. Cross-sectional profiles for each AFM images are shown.

the recovered pattern height of S2 (72 nm) correlates to a 65% recovery, whereas the S3 recovered pattern height (110 nm) correlates to an original pattern height of 80 nm prior to programming (Figures 3b and 3d). The partial recovery along S2 could be caused during the extended annealing at 60 °C and/or during the programming at 60 °C: i.e. the compression of the dense mold could have caused partial recovery of the grid pattern along S2 direction. Such mechanical loading induced shape recovery is possible due to the enhanced polymer chain mobility under the loading.[25] Such a long recovery time is likely associated with the long duration (30 min) to program the deformation, which is chosen because of the low pressure range of our imprinting equipment. In other words, if quick programming could be achieved with higher pressure, the recovery time at this corresponding temperature might also be correspondingly quick.

Line-and-space grating Nafion pattern was recovered after subsequently annealing the Nafion film at 90 °C for only 10 sec (Figure 3e), the height along S1 reaches 190 nm. However, a 10–15 nm height along S2 remained after the recovery, indicating a 86% recovery (100% × (110 nm–15 nm)/110 nm). Further annealing at 90 °C will cause the S2 to slowly disappear, but also induce noticeable reduction in S1. Finally, the line-and-space grating pattern completely smoothed out after annealing at 190 °C for 10 min, driven by the minimization of the surface energy of the Nafion. Therefore, a complete quadruple pattern memory effect is realized in the Nafion surface, counting the three temporary patterns (Figure 3) and the flat film.

This study reports the novel SMP ability to memorize and recover their lithographically fabricated, nanoscale surface patterns. The successful pattern memory cycle proved replicable for multiple pattern heights with 100% recovery using an acrylate-based SMP. Furthermore, a complete quadruple pattern memory is realized on a Nafion film surface. Note that the pattern memory effect shown here cannot be realized in regular thermoplastics such as polystyrene due to the lack of mechanism to store the elastic energy. Our study offers exciting potential applications of SMPs beyond their current focus of harvesting the macroscopic scale deformation for structural applications. Further, repeatedly program and recovery using NIL on the same permanent pattern is feasible, but the number of circles that a given SMP pattern is able to achieve remains to be determined. Lastly, no noticeable aging or dimensional change of the programmed pattern is observed after its storage at room temperature for 6 months.

This nanoscale pattern memorizing surface technology offers obvious advantages. For example, the significant reduction of

the SMP's active volume might lead to faster recovery rate and higher sensitivity. Most significantly, the pattern memorizing surface incorporates multi-functionality into SMP applications beyond conventional, structural usage. Examples for potential applications include harvesting optical responses for sensing and switching; surface and interfacial energies for controlling adhesion,[26,27] wetting of liquids,[28] alignment of liquid crystals,[29,30] and contact guidance of biological cells.[28,31,32] Both permanent and temporary patterns are defined by the NIL process and therefore can be tailored to meet specific applications. For instance, such pattern-memorizing surface can be used as smart coating that can change their reflectance/transmission upon triggering. Finally, the approach demonstrated here facilitates cost-effective, mass production, especially when utilizing the roll-to-roll (R2R) NIL process,[33] and applies to a wide range of SMP materials, rendering it a truly adaptive, technological platform.

Experimental Section

Acrylate-based SMPs were cured from monomer solution consisting of methyl methacrylate (MMA), poly(ethylene glycol dimethacrylate) (PEGDMA with molecular weight of 750, crosslinker,), and 2,2–dimethoxy–2-phenylacetodphenone (photo initiator).[20] In this study, the ratio between MMA and PEGDMA is 60/40. The crosslinked bulk SMP has a T_g of 95 °C, and a glass transition zone of 70 °C–110 °C, determined from the Dynamic Mechanical Analysis (DMA) measurements (Figure S1).

The series of SMP permanent patterns with identical pitch (Λ = 834 nm, line-to-space ratio R_{ls} = 1) but varying heights were replicated via SF-NIL on PAA patterns. As shown in Figure S2, such PAA grating patterns (identical pitch, sinusoidal line profile, but varying pattern heights) were first fabricated by controlled thermal reflow of as-imprinted PAA patterns. The SMP monomer solutions were then deposited onto the PAA patterns and photo-crosslinked for 15 min with an energy density approximately 10 mW/cm^2. Finally, the PAA patterns were dissolved in DI water to obtain the SMP replicas.

Nafion 117CS membranes (each ~100 cm^2) were purchased from Fuel Cell Store and used as received without any treatment such as pre-annealing. The glass transition region was determined to be from 55 to 140 °C (Figure S7) by DMA with a scanning rate of 1 °C/min. A piece of Nafion membrane (30 mm × 30 mm) was placed on top of a silicon wafer to function as a substrate and subsequently deformed by NIL.

All TE-NIL processes were performed on a nanoimprinter (Eitrie 3, Obducat). Two line-and-space grating molds (Si with a native layer of SiO_x), each having a line-to-space ratio of 1, were used. One of the molds had a pitch of 150 nm with a cavity depth of 45 nm and the other mold had a pitch of 834 nm, with a cavity depth of 194 nm. The molds were cleaned using piranha solution prior to use. After the piranha solution treatment, a low surface energy self-assembled monolayer of $CF_3(CF_2)_5(CH_2)_2SiCl_3$ (tridecafluoro-1,1,2,2-tetrahydrooctyltrichlorosilane, Sigma-Aldrich) was deposited on each mold by vapor deposition to facilitate mold release from the replicas after imprinting. Fabrication and programming procedures are presented in detail throughout the corresponding discussions for each test. Topographical morphologies of all samples at each stage of the pattern memory cycle were examined by AFM (Dimension 3100, Vecco) and FE-SEM (JSM-7401, JEOL).

Supporting Information

Supporting Information is available from the Wiley Online Library or from the author.

Acknowledgements

We acknowledge the funding support from National Science Foundation under the Grant No. CMMI-1031785 and ACS-PRF 50581-DNI7.

Received: April 26, 2011
Revised: June 2, 2011
Published online: July 8, 2011

[1] A. Lendlein, H. Y. Jiang, O. Junger, R. Langer, *Nature* **2005**, *434*, 879.
[2] Y. P. Liu, K. Gall, M. L. Dunn, A. R. Greenberg, J. Diani, *Int. J. Plast.* **2006**, *22*, 279.
[3] NASA, *NASA Tech Briefs* **2007**, *31*, 20.
[4] C. Liu, H. Qin, P. T. Mather, *J. Mater. Chem.* **2007**, *17*, 1543.
[5] M. Behl, A. Lendlein, *Mater. Today.* **2007**, *10*, 20.
[6] W. M. Huang, B. Yang, L. An, C. Li, Y. S. Chan, *Appl. Phys. Lett.* **2005**, *86*, 114105.
[7] H. J. Qi, T. D. Nguyen, F. Castroa, C. M. Yakacki, R. ShandaSa, *J. Mech. Phys. Solids.* **2008**, *56*, 1730.
[8] F. Castro, K. K. Westbrook, K. N. Long, R. Shandas, H. J. Qi, *Mech. Time-Depend. Mater.* **2010**, *14*, 219.
[9] F. Yang, E. Wornyo, K. Gall, W. P. King, *Nanotechnology* **2007**, *18*, 285302.
[10] B. A. Nelson, W. P. King, K. Gall, *Appl. Phys. Lett.* **2005**, *86*, 103108.
[11] K. A. Burke, P. T. Mather, *J. Mater. Chem.* **2010**, *20*, 3449.
[12] Y. F. Ding, H. W. Ro, J. F. Douglas, R. L. Jones, D. R. Hine, A. Karim, C. L. Soles, *Adv. Mater.* **2007**, *19*, 1377.
[13] Z. Fakhraai, J. A. Forrest, *Science* **2008**, *319*, 600.
[14] N. Liu, Q. Xie, W. M. Huang, S. J. Phee, N. Q. Guo, *J. Micromech. Microeng.* **2008**, *18*, 027001.
[15] W. Huang, N. Liu, X. Lan, J. Lin, J. Pan, J. Leng, S. Phee, H. Fan, Y. Liu, T. H. Tong, *Mater. Sci. Forum* **2009**, *614*, 243.
[16] Y. J. Zhang, Y. T. Cheng, D. S. Grummon, *Appl. Phys. Lett.* **2006**, *89*, 041912.
[17] S. Y. Chou, P. R. Krauss, P. J. Renstrom, *Science* **1996**, *272*, 85.
[18] J. L. Guo, *Adv. Mater.* **2007**, *19*, 1.
[19] T. C. Bailey, S. C. Johnson, S. V. Sreenivasan, J. G. Ekerdt, C. G. Willson, D. J. Resnick, *J. Photopolym Sci. Technol.* **2002**, *15*, 481.
[20] C. M. Yakacki, R. Shandas, C. Lanning, B. Rech, A. Eckstein, K. Gall, *Biomaterials* **2007**, *28*, 2255.
[21] T. Xie, *Nature* **2010**, *464*, 267.
[22] M. Behl, I. Bellin, S. Kelch, W. Wagermaier, A. Lendlein, *Adv. Funct. Mater.* **2009**, *19*, 102.
[23] I. Bellin, S. Kelch, R. Langer, A. Lendlein, *Proc. Natl. Acad. Sci. USA* **2006**, *103*, 18043.
[24] T. Xie, X. C. Xiao, Y. T. Cheng, *Macromol. Rapid Commun.* **2009**, *30*, 1823.
[25] H. N. Lee, K. Paeng, S. F. Swallen, M. D. Ediger, *Science* **2009**, *323*, 231.
[26] E. P. Chan, E. J. Smith, R. C. Hayward, A. J. Crosby, *Adv. Mater.* **2008**, *20*, 711.
[27] N. J. Glassmaker, A. Jagota, C. Y. Hui, W. L. Noderer, M. K. Chaudhury, *Proc. Natl. Acad. Sci. USA* **2007**, *104*, 10786.
[28] Y. F. Ding, J. R. Sun, H. W. Ro, Z. Wang, J. Zhou, N. J. Lin, M. T. Cicerone, C. L. Soles, S. Lin-Gibson, *Adv. Mater.* **2011**, *23*, 421.
[29] B. S. Zhang, F. K. Lee, O. K. C. Tsui, P. Sheng, *Phys. Rev. Lett.* **2003**, *91*, 215501.
[30] Y. Yi, M. Nakata, A. R. Martin, N. A. Clark, *Appl. Phys. Lett.* **2007**, *90*, 163510.
[31] M. J. Dalby, N. Gadegaard, R. Tare, A. Andar, M. O. Riehle, P. Herzyk, C. D. W. Wilkinson, R. O. C. Oreffo, *Nat. Mater.* **2007**, *6*, 997.
[32] K. A. Davis, K. A. Burke, P. T. Mather, J. H. Henderson, *Biomaterials* **2011**, *32*, 2285.
[33] S. H. Ahn, L. J. Guo, *ACS Nano* **2009**, *3*, 2304.